

1. Introduction

LS 5039 is one of the few known γ -ray binaries in the Galaxy. All these systems belong to the high-mass X-ray binary (HMXB) population, but they are peculiar examples of the HMXBs with the energy output dominated by emission in the high-energy (GeV) γ -ray band. The nature of this peculiarity is not completely understood yet. At least one system, PSR B1259-63 is known to be powered by a young pulsar (Johnston et al. 1992). The nature of the compact objects orbiting massive stars in other systems is not constrained. However, similarity of the spectral characteristics of the known γ -ray binaries suggests similar nature of the compact objects in these systems (see Dubus (2013) for a review). The current knowledge of the mass of the compact object is consistent with both neutron star and black hole possibilities (Moldón et al. 2012). The compact object moves close to the surface of the massive star, with the orbital separation at the periastron being just about twice the radius of the companion O star, growing to four stellar radii at the apastron. The compact object always moves through a denser part of the stellar wind and pulsed radio emission from the putative young pulsar in the system could not be detected because of the strong free-free absorption.

LS 5039 is observed in a very broad energy range from radio up to TeV energy band. Both X-ray and TeV emission are modulated on the orbital time scale, with a maximum close to the phase of inferior conjunction of the orbit (Aharonian et al. 2006; Takahashi et al. 2009). To the contrary, the GeV γ -ray emission, detected by *Fermi* reveals a different orbital modulation pattern, with a pronounced maximum at the periastron and a suppression of the flux at the inferior conjunction (Abdo et al. 2009).

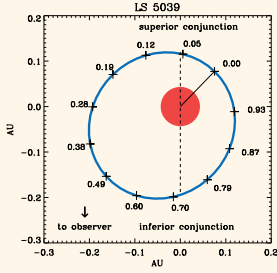


Figure 1: The binary orbit of LS 5039 as seen from directly above, from Dubus (2013)

Explanation of both variability patterns, as well as of the energy dependence of the variability pattern provides a challenge for phenomenological models of the source. In the current work we present our analysis of the 59 month of *Fermi* observations of LS 5039 in the 60 MeV – 300 GeV energy range. We use this wealth of data to study the spectral variability of the source at different orbital phases in order to put constraints on the origin of the relativistic electrons. Basing on these observations we propose two-zone self-consistent model that allows to explain observable GeV orbital modulation as well as a correlation between keV-TeV energy bands.

2. Data analysis and results

For the *Fermi*/LAT (Atwood et al. 2009) analysis we consider 59 months of the data (August, 4th, 2008 – July, 4th, 2013), that results in ~ 2 times better statistics in comparison with earlier works (Abdo et al. 2009; Hadasch 2012). We restrict the analysis to energies 60 MeV – 300 GeV at which templates for galactic and extragalactic diffuse backgrounds are available. Due to rapid increase of the *Fermi*/LAT point spread function (PSF) at energies < 100 MeV at which PSF $> 15^\circ$, we split the analysis into two, high (> 100 MeV) and low (60-100 MeV) energy parts. For high energies we consider the $30^\circ \times 30^\circ$ region around the LS 5039 position (in J2000 coordinates). For the analysis at energies below 100 MeV we consider broader, $60^\circ \times 60^\circ$ region around LS 5039 position and P7CLEAN_V6: :FRONT class photons to account for significantly larger *Fermi*/LAT PSF. In both cases the model of the region includes standard templates for galactic and extragalactic diffuse backgrounds as well as all sources from 2 years (2FGL) *Fermi* catalog, Nolan et al. (2012) in the region.

The increased exposure time allowed us to analyse the spectrum in more details than it was done in previous works. It turned out that while at energies > 1 GeV the spectrum is almost unchanged with the orbital phase, low energy part demonstrates much more significant variability. This can be clearly seen in the orbital folded light curves at different energies are shown in Fig. 3. In lowest energy band (60-100 MeV) the light curve demonstrates behaviour similar to X-rays and TeVs energy band, (Kishishita et al. 2009; Aharonian et al. 2005) with the minimum at phase ~ 0.2 . At higher energies (> 100 MeV) the minimum shifts to phases 0.5 (at 100 MeV–1 GeV) and 0.75 (1–3 GeV) in agreement with Abdo et al. (2009). We also would like to note, that the ratio between maximal and minimal flux along the orbit decreases with energy. For 60-100 MeV this ratio is ~ 5 , while it is only ~ 1.5 for 1–3 GeV.

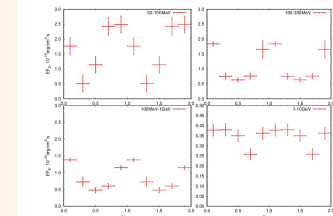


Figure 3: The flux of LS 5039 at different energy bands as function of orbital phase. At low (50-100 MeV) energies the light curve is similar to one observed in X-rays and TeVs, while at 100 MeV–3 GeV is similar to observed previously in γ -rays by Abdo et al. (2009)

3. Interior of the binary system

Consider first the time-averaged spectral properties of emission coming from an internal layer located at a certain range of distances $d \sim (1.5...2.5)R_*$ from the massive star. The broad band emission from the system consists of the synchrotron and IC components. The seed photons for the IC scattering are coming from the massive star of the temperature $T_* \sim 3 \times 10^4$ K, have typical energy $\epsilon_* \approx 3T_* \approx 10$ eV. The strength of the magnetic field with the energy density in equipartition with the radiation energy density is

$$B_{eq} = (8\pi U_{rad})^{1/2} \approx 1.5 \times 10^2 \left[\frac{T_*}{3 \times 10^4 \text{K}} \right]^2 \left[\frac{d}{2R_*} \right]^{-1} \text{G} \quad (1)$$

In such magnetic field, the fluxes of synchrotron and IC emission by the same electrons should be equal. The energy band in which electrons with energy $E_e \sim 30$ GeV are emitting synchrotron radiation is $\epsilon_s \approx 5 \times 10^3 \left[\frac{B}{100 \text{G}} \right] \left[\frac{E_e}{3 \times 10^{10} \text{eV}} \right]^2 \text{eV}$

In the photon field of the massive star same 30 GeV electrons will produce gamma radiation at $\epsilon_{IC} \approx 10 \text{GeV}$. Comparing the observed source energy flux at 5 keV and in the high-energy γ -ray band, at 10 GeV, one finds that the fluxes in the two bands are comparable, see Fig. 4. This means that the magnetic field strength inside the binary system is close to the equipartition value given by Eq. (1).

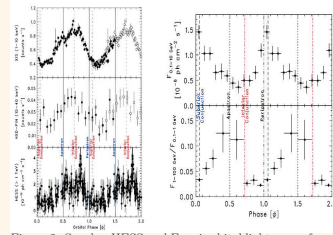


Figure 2: Suzuki, HESS and Fermi orbital lightcurves from (Takahashi et al. 2009; Abdo et al. 2009)

- Comparing gyroradius of high-energy electrons R_L to the synchrotron cooling distance D_s one find that the ratio

$$\frac{D_s}{2\pi R_L} = 5 \times 10^3 \left[\frac{B}{100 \text{G}} \right]^{-1} \left[\frac{E_e}{3 \times 10^{10} \text{eV}} \right]^{-2} \quad (2)$$

becomes comparable to one at the energy $E_{e,max} \approx 3 \times 10^{12} \left[\frac{B}{100 \text{G}} \right]^{-1/2} \text{eV}$

- At the energies above $E_{e,max}$ electrons could not be efficiently accelerated in situ to the energies much higher than this limiting energy. Thus, $E_{e,max}$ should be considered as an order-of-magnitude estimate of the maximal attainable energy for high-energy electrons in the system.
- Electrons accelerated to the maximal attainable energy emit synchrotron radiation in the energy band $\epsilon_{s,max} \approx 5 \times 10^7 \left[\frac{B}{100 \text{G}} \right] \left[\frac{E_{e,max}}{3 \times 10^{12} \text{eV}} \right]^2 \text{eV} \approx 5 \times 10^7 \text{eV}$
- The limiting energy of the quanta of synchrotron radiation does not depend on the magnetic field strength, the phenomenon called self-regulated cut-off[†] of the synchrotron spectrum (Aharonian 2000).
- The estimate of the energy of the self-regulated cut-off of the synchrotron emission is close to the observed value of the cut-off of the orbital phase modulated component of the high-energy γ -ray spectrum, see Figs. 3 and 4.
- LS 5039 system works in the "extreme efficiency" acceleration regime and the modulated component is being due to the synchrotron emission from the interior of the binary system.

4. Orbital variability of synchrotron component

- The synchrotron cooling distance $D_s = 4 \times 10^{10} \left[\frac{B}{100 \text{G}} \right]^{-2} \left[\frac{E_e}{3 \times 10^{10} \text{eV}} \right]^{-1} \text{cm}$ is much shorter than the size of the system, so that the highest energy electrons efficiently loose energy before escaping from the source.
- Assuming that the injected power is roughly constant and that adiabatic and inverse Compton energy losses in the deep Klein-Nishina regime are sub-dominant for the highest energy particles, independently of the orbital phase (this is true in the compact pulsar wind nebula model of the source), the only change in the pattern of the synchrotron emission could be the shift of the spectrum toward higher/lower energies, in response to the increase/decrease of the magnetic field strength, as shown in Fig. 3.
- Maximum of the synchrotron emission in the energy band above 100 MeV is observed around the periastron, where magnetic field is the strongest and the synchrotron spectrum shifts toward higher energies so that it enters well into the $E > 100$ MeV band.
- Shift of the synchrotron spectrum toward higher energies leads to the decrease of the X-ray flux close to the periastron.
- The overall shape of the TeV band light curve could be satisfactory explained by a combination of the orbital phase dependent effects of the anisotropic IC scattering and pair production. In addition increasing magnetic field close to the periastron leads to stronger synchrotron loss and to the suppression of the IC emission.

5. Broad band SED and spectral components

- If high-energy particles leave the region in the interior of the binary orbit with $v_{esc} \sim c$, then t_s and t_{IC} larger than t_{esc} at energies below 3 GeV. In case of slow escape with the stellar wind synchrotron cooling time is larger than escape time only for electrons with energies below 30 MeV.
- Electrons with low energies could spread around the system and produce extended synchrotron and IC emission on much larger distance scales, as observed in the radio band on the distance scales of 100 R_* .
- Case of slow escape could be immediately ruled out, because in this case the 30 MeV electrons could produce radio synchrotron emission in the nebula only if $B_{nebula} > 100 \text{G}$.
- The IC emission of the larger scale nebula filled with electrons with energies $E < 3$ GeV reaches the energy 300 MeV and should be visible to Fermi.
- This extended nebular IC emission is only weakly modulated on the orbital time scale, because of the very large size of extended emission region, where the radiation and magnetic field are weaker and the cooling times of electrons become increasingly longer.
- The extended nebula also loses high-energy electrons because of the escape to still larger distances.
- In case of fast escape, even the highest energy, 3 GeV electrons would not be able to cool efficiently in the nebula and produce any significant synchrotron and IC flux.
- Even for slow escape electrons with energies below 300 MeV could not be efficiently cooled in the nebula and escape toward still larger distances. This leads to the suppression of synchrotron power at the energies below GHz, as observed by GMRT (Bhattacharyya et al. 2012).

6. Conclusions

- Search for the orbital modulation of LS 5039 in *Fermi*/LAT data reveals different dependences of the flux on orbital phase for different energy bands.
- At low (< 100 MeV) energies flux demonstrates strong variability with the minimum at orbital phase 0.3, close to one observed in X-rays and TeVs.
- With increase of the energy, the minimum shifts toward the orbital phase 0.5 – 0.7, observed previously in GeV range.
- Simultaneously with the increase of energy the significance of the variability decreases.
- The observed orbital folded light curves can be interpreted as a sum of steady (dominant at GeV energies) and significantly variable (dominant at lower energy) components.
- These components are readily explained in terms of proposed two-component model. In this model variable component is explained by synchrotron emission from the interior part of the binary, while the steady one is the IC counterpart of extended radio synchrotron emission from a much larger than the binary system size region.

References

- Abdo, A. A., Ackermann, M., Ajello, M., et al. 2009, *ApJ*, 706, L56
 Aharonian, F., Akhperjanian, A. G., Aye, K.-M., et al. 2005, *Science*, 309, 746
 Aharonian, F., Akhperjanian, A. G., Bazer-Bachi, A. R., et al. 2006, *A&A*, 460, 743
 Aharonian, F. A. 2000, *New A*, 5, 377
 Aharonian, F. A., Belyanin, A. A., Derishev, E. V., Kocharovskiy, V. V., & Kocharovskiy, V. V. 2002, *Phys. Rev. D*, 66, 023005
 Atwood, W. B., Abdo, A. A., Ackermann, M., et al. 2009, *ApJ*, 697, 1071
 Bhattacharyya, S., Godambe, S., Bhatt, N., Mitra, A., & Choudhury, M. 2012, *MNRAS*, 421, L1
 Dubus, G. 2013, *A&A Rev.*, 21, 64
 Hadasch, D. 2012, *International Journal of Modern Physics Conference Series*, 8, 61
 Johnston, S., Manchester, R. N., Lyne, A. G., et al. 1992, *ApJ*, 387, L37
 Kishishita, T., Tanaka, T., Uchiyama, Y., & Takahashi, T. 2009, *ApJ*, 697, L1
 Moldón, J., Ribó, M., & Paredes, J. M. 2012, *A&A*, 548, A103
 Nolan, P. L., Abdo, A. A., Ackermann, M., et al. 2012, *ApJS*, 199, 31
 Takahashi, T., Kishishita, T., Uchiyama, Y., et al. 2009, *ApJ*, 697, 592